Paper No.
13004

NACE INTERNATIONAL
CORROSION Conference & Expo 2019

Effect of Alkyl Tail Length on CMC and Mitigation Efficiency Using Model Quaternary Ammonium Corrosion Inhibitors

Negar Moradighadi, Starr Lewis, Juan M. Domínguez Olivo, David Young, Bruce Brown, Srdjan Nesic
Institute for Corrosion and Multiphase Technology
Department of Chemical & Biomolecular Engineering
Ohio University
Athens, OH 45701

ABSTRACT

Application of inhibitors is an established and cost-effective method to mitigate internal corrosion of mild steel pipelines in the oil and gas industry. Conventionally, surfactant-type organic inhibitors are frequently applied based on their critical micelle concentration (CMC) values and their adsorption to mild steel evaluated based on laboratory tests that show a reduction in corrosion rate. In this work, the relationship between reduction in corrosion rate, CMC and inhibitor surface saturation concentration on mild steel was studied using model quaternary ammonium inhibitors with different alkyl tail lengths. The quaternary ammonium model compounds were synthesized in-house and characterized by ^{1}H-NMR before their use. Their CMCs were determined using surface tension measurements. Results showed that, although the CMC value and surface saturation concentration were the same for two of the inhibitors tested, there was no relationship observed between measured CMC values, surface saturation concentrations, and the calculated corrosion efficiencies for the five model inhibitor compounds tested. Consequently, using CMC values as a measurement for injection of inhibitors might not be considered as a reliable factor.

INTRODUCTION

Corrosion is broadly defined as deterioration of materials due to chemical reactions between metal and an aggressive environment.[1] Corrosion can lead to severe, and frequently unrecognized, economic losses.[2] Concerning the upstream oil and gas industry, internal pipeline corrosion is considered both an economic and a safety problem. Because of this, many studies have investigated the mechanisms, conditions and flow patterns responsible for pipeline corrosion.[3–7] Among different corrosion mitigation strategies, the most used and cost-effective corrosion mitigation method is by continuous injection or batch treatment of corrosion inhibitor in production pipelines.

Inhibitors are chemical compounds which can protect a metal surface either by the formation of a protective film layer or by reducing the corrosivity of an aggressive environment.[1, 8–10] Organic corrosion inhibitors have a charged head group which can adsorb on the metal surface and a hydrophobic tail which can retard the presence of water molecules. Generally, the mechanism of corrosion mitigation by organic inhibitors is *via* formation of a protective film layer by adsorption of the inhibitor molecules on the metal surface that retards the corrosive species from interacting with the metal. [11–13]

Although coverage of a metal surface by inhibitor molecules is considered as a barrier against corrosive species, the actual mechanism of protection is not akin to a solid impenetrable layer being present. In contrast with the assumption that surface coverage retards all electrochemical reactions on the surface of a metal, potentiodynamic polarization experiments have shown that the presence of inhibitors on a metal surface does not affect the mass transfer limiting current of the hydrogen evolution reaction.[14] Moreover, a study using Atomic Force Microscopy (AFM) on a mild steel surface in the presence of an inhibited solution did not seem to correlate with associated corrosion studies using the same mild steel and same inhibitor. Although AFM results had shown surface topography in the nanometer range where the corrosion inhibitor, at 1 CMC value, seemed to fully cover the surface of the metal, the calculated efficiency in the associated corrosion studies was less than 80%.[12]

With continued research, more has been learned about how the alkyl tail length of a corrosion inhibitor influences an inhibitor's efficiency. Some studies over the past decade have reported that the length of the alkyl tail of a corrosion inhibitor governs, and is proportional to, the extent of adsorption of corrosion inhibitor on the metal surface and amount of surface coverage obtained.[15–18] A more recent study agreed that inhibitor efficiency was proportional to inhibitor alkyl tail length, and was able to provide a more fundamental mechanistic view of surface coverage.[19] This study found that an increase in the alkyl tail length of a model inhibitor increased the activation energy for charge transfer, such as the dissolution of iron. Although constrained by the solubility limit of inhibitor components, an increase in the alkyl tail length of an adsorbed inhibitor increases the activation energy for charge transfer which occurs at the metal surface and, therefore, retards the corrosion rate accordingly.

Conventionally, surfactant-type organic inhibitors are frequently applied based on their critical micelle concentration (CMC). In many research studies, it has been assumed that at a concentration equal to or above the CMC, the surface of the metal would be fully covered by corrosion inhibitor molecules and result in the maximum reduction of corrosion rate.[20–22] But the surface tension measurements used for most CMC evaluations are conducted at the air/solution interface, which may not necessarily have a direct relationship to the inhibitor coverage at the metal/solution interface.

The primary objective of this research was to determine the relationship between CMC, metal surface saturation concentration and reduction in corrosion rate with respect to the alkyl tail length. This objective was completed by explicitly using model benzyldimethylalkylammonium bromide compounds which were synthesized and characterized prior to their use.

EXPERIMENTAL METHODOLOGY

Synthesis of Quaternary Alkylammonium Bromide Inhibitor Model Compounds (QABs)

Benzyldimethylalkylammonium bromides with five different alkyl tail lengths have been synthesized. N,N-Dimethylbenzylamine was used as the tertiary amine, undergoing quaternization in the presence of an equivalent stoichiometric amount of an alkyl bromide. Acetonitrile was chosen as the solvent as it was reported to achieve high amine quaternization rates.[23, 24] The critical parameters for synthesizing the model quaternary alkylammonium bromide (QAB) compounds for corrosion inhibition studies are shown in Table 1. The name "K2-Cx" was derived from previous research with a quat-type inhibitor, known in-house as "K2", and the "Cx" corresponds to the x alkyl group constituting the tail of the molecule.

Table 1

Parameters for Synthesizing QABs

QAB	Amine	Alkylating Agent	Solvent	Reflux Temperature	Duration
K2-C6	N,N-Dimethylbenzylamine ($C_9H_{13}N$)	$C_6H_{13}Br$	CH_3CN	82°C	24 hours
K2-C8		$C_8H_{17}Br$			
K2-C10		$C_{10}H_{21}Br$			
K2-C12		$C_{12}H_{25}Br$			
K2-C14		$C_{14}H_{29}Br$			

The experimental setups for synthesis and recovery of the QAB compounds are shown in Figure 1. The dimethylbenzylamine (equivalent to 0.100 moles) and acetonitrile (100 mL) were added into a 500 ml two-necked round-bottom flask, a condenser was then attached and, finally, an addition funnel containing the alkyl bromide (also equivalent to 0.100 moles) was inserted into the second neck. The round-bottom flask was then heated to the reflux temperature (82^{o}C) by an appropriately sized heating mantle connected to a Variac[†]. The flow of water in the condenser ensured reflux of the acetonitrile/amine mixture. After refluxing commenced, the alkyl bromide was added to the system dropwise using the addition funnel (Figure 1.a). Reflux was maintained for a further 24 hours. After the quaternization reaction was completed, the solvent was removed from the system by rotary evaporation (rotovaping) (Figure 1.b).

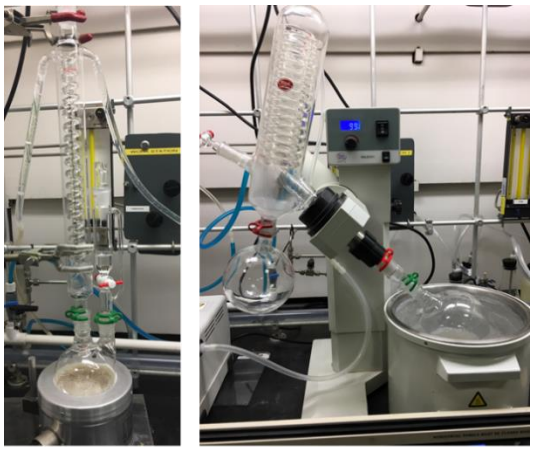

Figure 1: a) Reflux system for amine alkylation. b) Recovery of products by rotary evaporation.

The structure and purity of the synthesized inhibitor model compounds were confirmed by ^{1}H-NMR spectroscopy. Melting point measurements were also obtained. The K2-C4 and K2-C16 used in the experiments were synthesized as described elsewhere.[19]

[†] Trade Name

Critical Micelle Concentration Measurements

With the increase in inhibitor concentration in an aqueous solution, the solution/air interfacial tension decreases until it approaches a constant value (i.e., its variation is within the measurement error), believed to correspond to the onset of micelle formation in the bulk and is called the critical micelle concentration (CMC). To determine the CMC, the solution/air surface tension was measured as a function of inhibitor and salt concentrations. The Du Noüy ring method was used in the current work because of its higher accuracy for surface tension measurement compared to other methods, such as the drop weight method. In the Du Noüy ring method, the force required to pull the ring out from the solution/air interface was related to the interfacial tension as calculated by Equations (1) and (2).[25, 26]

$$\sigma = \frac{F}{p\cos\theta} f \tag{1}$$

$$f = 0.725 + \left(\frac{0.00363\sigma}{\pi^2 R^2 (D-d)} - \frac{1.679r}{R} + 0.04534\right)^{1/2} \tag{2}$$

Where:
σ: Surface tension (mN/m)
F: Force required to pull out the ring from the interface (N)
p: The wetted length of the ring which is the sum of the inner and outer circumference (cm)
θ: The contact angle between the ring and the liquid
f: Correction factor
D: Density of the lower phase (g/cm^3)
d: Density of the upper phase (g/cm^3)
R: The radius of the ring (cm)
r: The radius of the wire of the ring (cm)

Two simplifications were used in this equation. First, the contact angle between water and the platinum ring was considered to be zero due to its high wettability [27] so that $\cos(\theta) = 1$. Second, the density of air was considered negligible with respect to the density of water, so that $(D-d) = 1$ g/cm^3.

Test Condition and Procedures

The procedure for CMC measurements of the inhibitor model compounds was initiated by preparing solutions with different concentrations using series dilution. Each solution was prepared by having a defined inhibitor concentration based on the volume of deionized water, then certified ACS grade NaCl was added to create the desired salt concentration in each container. The parameters for the CMC measurements are shown in Table 2.

Table 2

Test Matrix for CMC Measurements

Parameters	Value
Inhibitor Model Compounds	K2-C4, K2-C6, K2-C8, K2-C10, K2-C12, K2-C14, K2-C16
Solvent	Water
NaCl concentration (wt.%)	0, 1, 10
Temperature (^{o}C)	30

Prior to each measurement, the ring was cleaned using acetone, deionized water and finally it was passed through a flame for 2-3 seconds. The surface tension of the solution was then measured two or three times with the Krüss[‡] K20 tensiometer using the Du Noüy ring method.

Effect of CO_2 on Critical Micelle Concentration

Effect of CO_2 on the CMC of K2-C14 was also investigated. The surface tension of the K2-C14 inhibitor solution at 1 wt.% NaCl was measured. In the following step, the same solution was sparged by CO_2 for 1 hour, and the surface tension of the solution was measured using the same method and compared to the unsparged solution surface tension.

Electrochemical Measurements

The following test methodology is the same as the procedure described by Dominguez, et al.[19] Corrosion rate measurements were obtained using an API 5L X65 steel rotating cylinder electrode (RCE) in a 2-liter glass cell, continuously purged with CO_2, as shown in Figure 2. The 3-electrode configuration included the RCE as the working electrode, a saturated Ag/AgCl reference electrode, and a platinum covered titanium mesh as the counter electrode. The linear polarization resistance (LPR) technique was used by polarizing the working electrode potential from -5 mV to +5 mV with respect to the open circuit potential. The corrosion rates were determined using a B value of 26 mV/decade. Table 3 shows the test matrix for corrosion rate measurements.

[‡] Trade Name

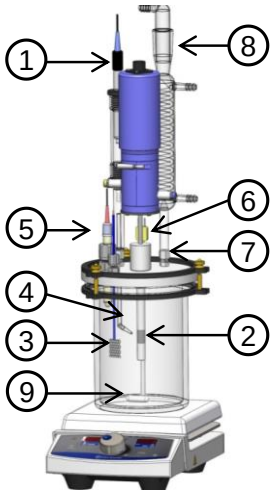

1. Reference Electrode (RE – Saturated Ag / AgCl)
2. Rotating Cylinder Electrode (WE)
3. Counter Electrode (CE)
4. Luggin Capillary
5. pH Meter
6. Thermocouple
7. Gas in
8. Gas out
9. Magnetic Stirrer

Figure 2: Glass cell set up used for corrosion experiments.[(1)]

Table 3

Test Matrix for Corrosion Rate Measurement in Presence of Inhibitors

Parameter	Value
Working electrode	UNS K03014 API 5L X65
RCE velocity	1000 rpm
Counter electrode	platinum covered titanium mesh
Reference electrode	Ag/AgCl
Temperature	30°C
pH	4.0 ± 0.1
Test solution	1 wt.% NaCl
Corrosion inhibitors and concentrations	K2-C4 (10, 50, 100, 150, 200, 250, 300 ppm v/v) K2-C8 (10, 50, 100, 150, 200, 250 ppm v/v) K2-C12 (10, 50, 100, 150, 200 ppm v/v) K2-C14 (5, 10, 25, 50, 100 ppm v/v) K2-C16 (5, 10, 25, 50 ppm v/v)
Duration	7 hours

RESULTS AND DISCUSSION

Synthesis of Quaternary Ammonium Compounds

Benzyldimethylalkylammonium bromides having five different alkyl tail lengths were synthesized. K2-C4 and K2-C16 used for the experiments were synthesized in prior research and their characterization data is shown elsewhere.[19] Based on the tail length of the synthesized compounds, they were either in a solid or ionic liquid state (Figure 3). Table 4 shows the states of the synthesized compounds and the range of melting points.

[(1)] Image courtesy of Cody Shafer, ICMT, Ohio University.

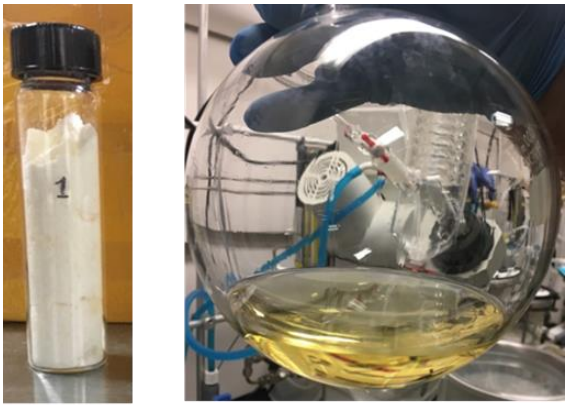

Figure 3: Synthesized inhibitors: a) K2-C6, crystalline solid; b) K2-C8, ionic liquid.

Table 4

Characterizations of the Synthesized Inhibitor Model Compounds

Compound	State of Mater	Melting Point Range (°C)
K2-C4	Crystalline solid	148 - 150.5
K2-C6	Crystalline solid	120.0 - 121.9
K2-C8	Ionic liquid	-
K2-C10	Ionic liquid	-
K2-C12	Ionic liquid	-
K2-C14	Waxy solid	63.7 - 67.0
K2-C16	Waxy solid	73.3 - 80

Based on the ^{1}H-NMR spectra of the products, it was found that the synthesized components have the desired structure. ^{1}H-NMR spectra indicate the products are free of acetonitrile (solvent) as well as bromoalkane and dimethylbenzylamine (reactants). Based upon the absence of other peaks, the purity of the products was above 99.5%. Figure 4 shows the ^{1}H-NMR spectra of K2-C6, K2-C8, K2-C10, K2-C12, K2-C14 inhibitors in the same manner which the ^{1}H-NMR spectra of K2-C4 and K2-C16 have been described elsewhere.[19]

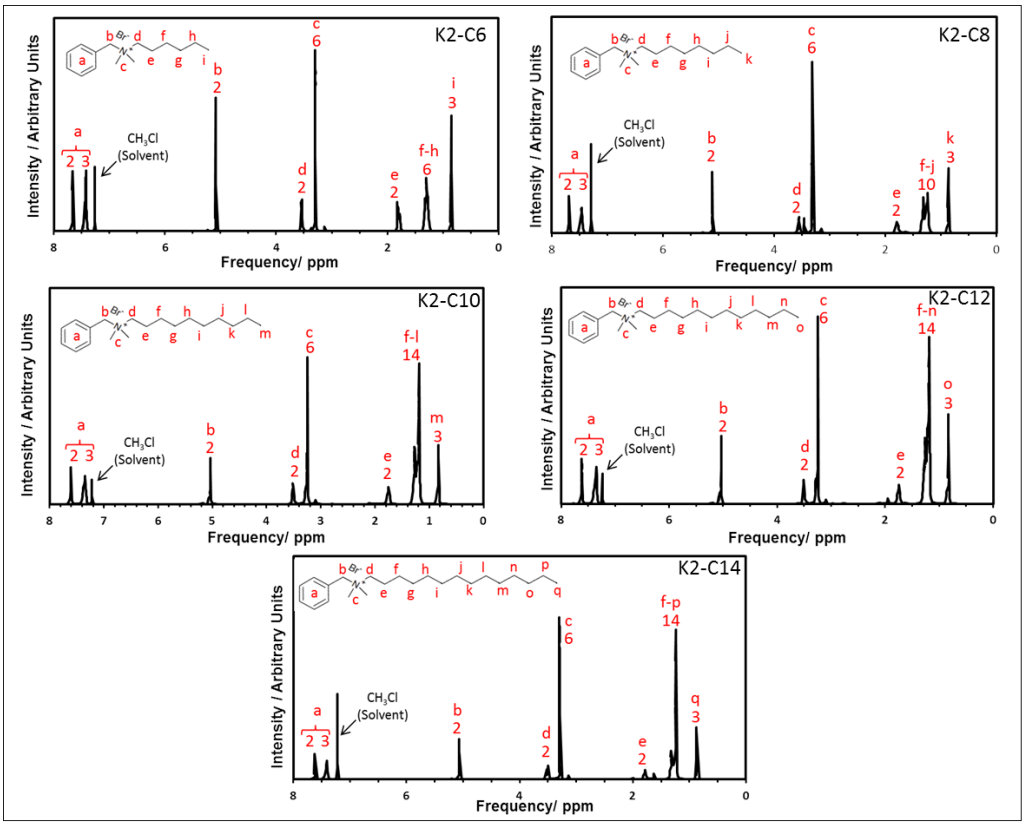

Figure 4: ^{1}H-NMR spectra of the synthesized inhibitors.

CMC Measurements of the Synthesized Inhibitor Model Compounds

Effect of CO_2 on Critical Micelle Concentration

The effect of CO_2 on CMC value of K2-C14 was determined by surface tension measurement. The CMC value of K2-C14 before and after sparging with CO_2 was investigated, and it has been concluded that the presence of CO_2 did not influence the measured CMC value. As shown in Figure 5, the intersection of the two lines for each test is considered to be approximately at the same CMC.

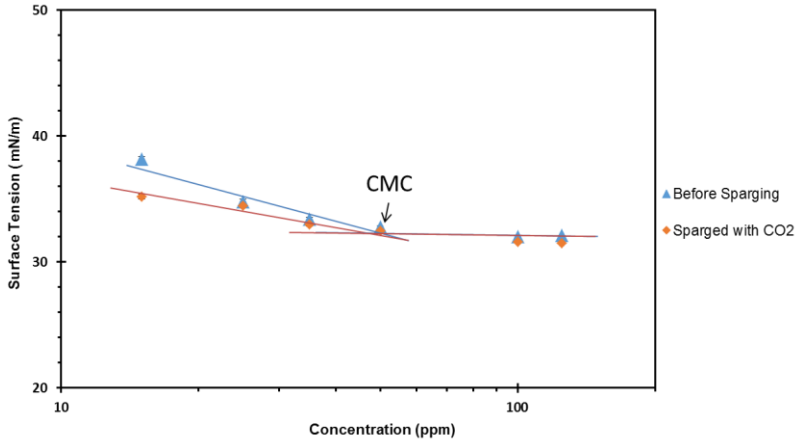

Figure 5: The surface tension of the inhibitor solution based on concentrations of K2-C14 in the presence of CO_2 and 1 wt.% NaCl. Size of error bars is smaller than the size of the data point markers.

Effect of Salt Concentration and Alkyl Tail Length of Corrosion Inhibitor on CMC

Surface tension measurement was used to determine the CMC values of the synthesized model compounds. Based on Figure 6, K2-C4, K2-C6, and K2-C8 did not have a CMC value at any of the measured salt concentrations. This was assumed to be due to the short alkyl tail length, which results in low hydrophobicity.

It was observed that increasing the salt content of the solution allowed micelles to form at lower inhibitor concentrations. As Figure 7 shows, K2-C10 did not have a measurable CMC value at 0 wt.% NaCl concentration; however, by increasing the salt concentration to 1 and 10 wt.%, CMC values were determined (Table 5).

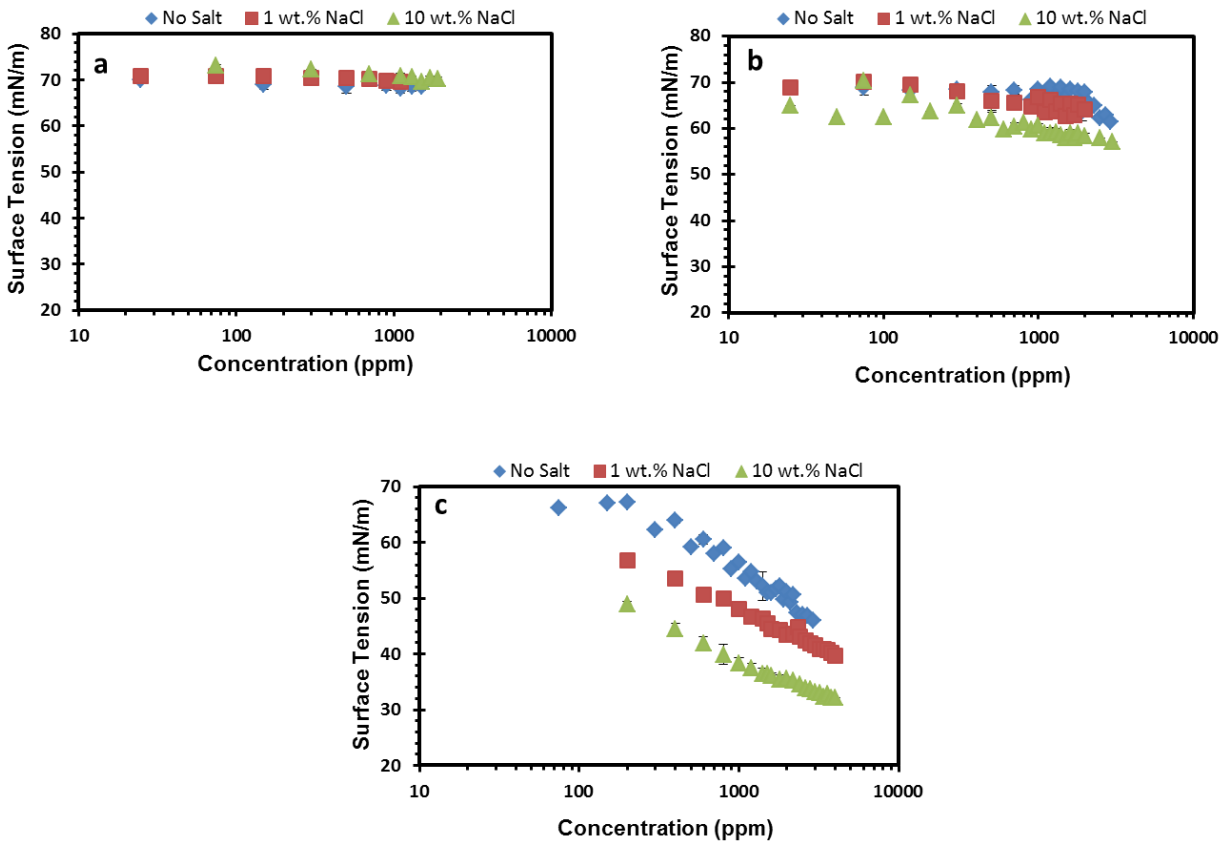

Figure 6: Surface tension measurements of model inhibitor compounds, a: K2-C4, b: K2-C6, c: K2-C8. Some of the error bars are smaller than the size of the data point markers.

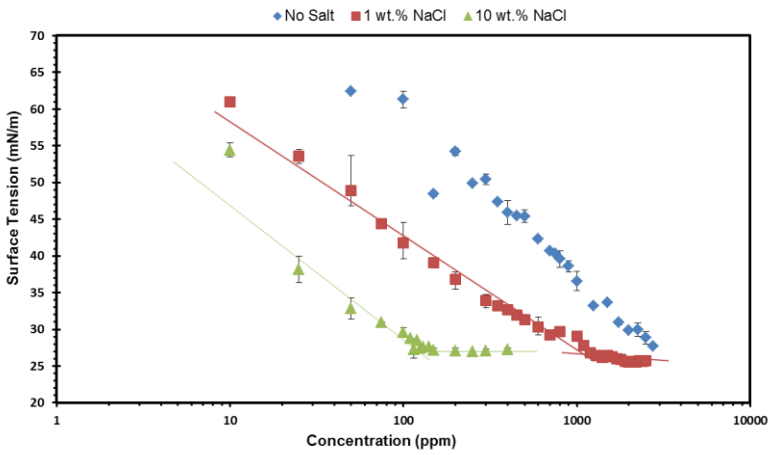

Figure 7: Surface tension measurements of K2-C10 in different salt solutions. Some of the error bars are smaller than the size of the data point markers.

The CMC values of K2-C12 and K2-C14 were determined and indicate that by increasing the alkyl tail length, the CMC values decreased due to an increase in hydrophobicity (Figure 8 and Figure 9). Table 5 shows the CMC values of the synthesized model compounds.

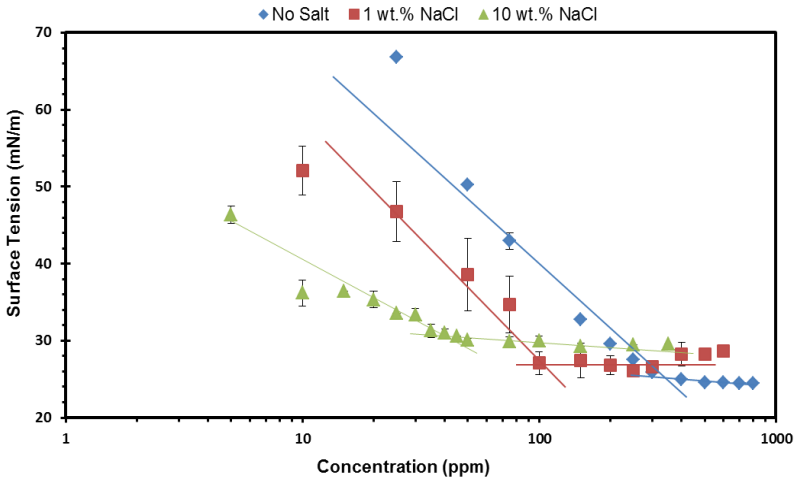

Figure 8: Surface tension measurements of K2-C12 in different salt solutions. Some of the error bars are smaller than the size of the data point markers.

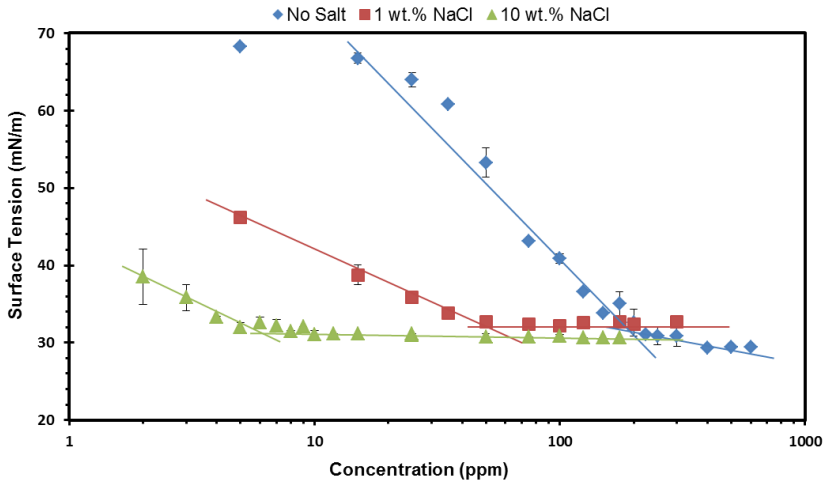

Figure 9: Surface tension measurements of K2-C14 in different salt solutions. Some of the error bars are smaller than the size of the data point markers.

By increasing the tail length of an inhibitor, its solubility in water decreases. Due to solubility limitations, the maximum concentration of K2-C16 in water was reached before its CMC value in pure water could be established. However, by increasing the salt concentration, the CMC values were determined for K2-C16 (Figure 10).

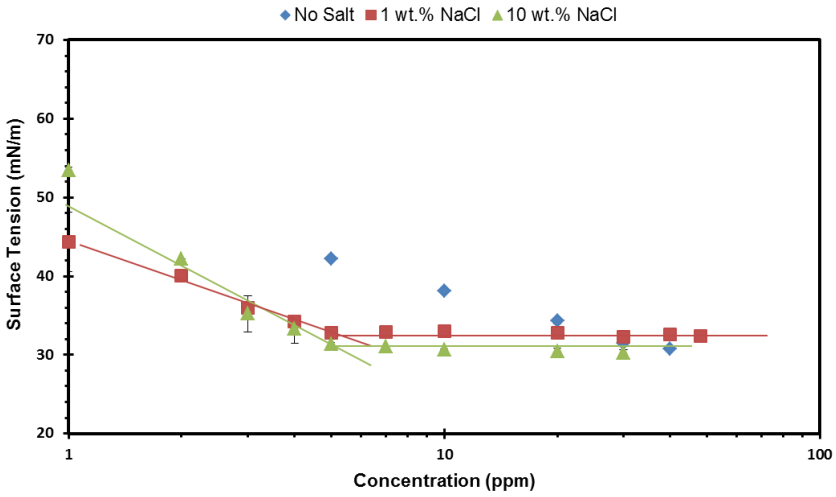

Figure 10: Surface tension measurements of K2-C16 in different salt solutions. Some of the error bars are smaller than the size of the data point markers.

Table 5

CMC Values of the Inhibitor Model Compounds (ppm)

Inhibitor Model Compound	0 wt.% NaCl	1 wt.% NaCl	10 wt.% NaCl
K2-C4	> 2000	> 2000	> 2000
K2-C6	> 3000	> 3000	> 3000
K2-C8	> 4000	> 4000	> 4000
K2-C10	> 3000	1250 ±50	123 ± 6
K2-C12	375 ± 25	116 ± 23	38 ± 5
K2-C14	191 ± 31	50 ± 5	6.2 ± 1.2
K2-C16	> 50	5.6 ± 0.9	5.5 ± 1.3

Correlation Between CMC and Reduction in Corrosion Rate

At 1 CMC and above, the number of inhibitor molecules should be at an approximately constant value at the gas/liquid interface since the surface tension is also approximately constant. It is assumed that inhibitors are attracted to the metal/liquid interface similar to the gas/liquid interface, then at 1 CMC a maximum concentration of adsorbed inhibitor would be reached for the same reason as above. So, there should be a correlation between the corrosion mitigation efficiency and the measured CMC values, i.e., that maximum efficiency should be reached at approximately 1 CMC.

Using a definition associated with inhibitor coverage at the metal/liquid interface, a maximum reduction in corrosion rate should be achieved when the surface of the metal is at maximum coverage by corrosion inhibitor. Murakawa, et al., defined this inhibitor concentration as the surface saturation concentration.[28] In recent research, Dominguez, et al., used the surface saturation concentration values to study the mechanisms of four of the same inhibitors characterized in this study.[19] Experiments for determination of the surface saturation concentration for the in-house synthesized model quaternary ammonium bromide corrosion inhibitors (K2-C4, K2-C8, K2-C12, K2-C14 and K2-C16) were conducted in a CO_2 corrosion environment, at pH 4 and temperature of 30^{o}C. By comparing these corrosion mitigation parameters with the CMC values for the same inhibitors, a correlation between the two should be observed.

Figure 11, shows corrosion rate measurement in the presence of K2-C14 at its different concentrations and at the test condition described. The surface saturation concentration was chosen based on the maximum efficiency of the tested inhibitor (25-50 ppm). The same procedure was performed to analyze the corrosion efficiency of the other tested inhibitors to obtain the surface saturation concentrations.[19]

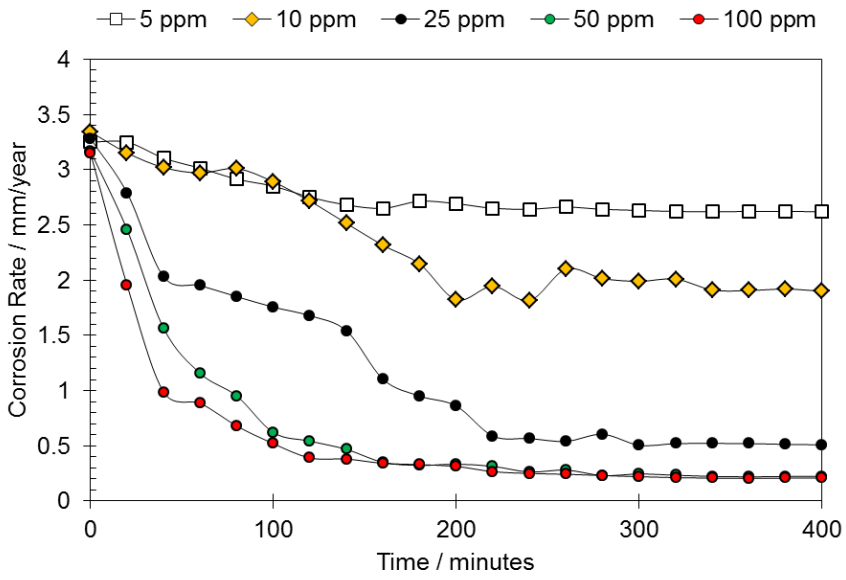

Figure 11: Independent corrosion rate measurements to determine the lowest concentration of inhibitor to attain maximum efficiency of K2-C14 (0.96 bar CO_2, 1 wt.% NaCl, pH 4, 30 ^{o}C, RCE at 1000 rpm).

Results in Table 6 show that, although no CMC value was detected for K2-C4 and K2-C8, for concentrations up to 2000 and 4000 ppm respectively, these inhibitors have surface saturation concentration values within the range of 100 to 200 ppm.[19] Interestingly, both K2-C12 and K2-C14 have similar values for CMC and surface saturation concentration. Although corrosion rate measurements for K2-C16 observed that there was no increase in mitigation efficiency between 50 and 100 ppm inhibitor concentrations, this is because the solubility limit for K2-C16 is 50 ppm. Therefore, the surface saturation concentration of K2-C16 is estimated to be above 50 ppm, which is higher than the CMC by a factor of 10. Overall, we can conclude that the correlation between CMC and reduction in corrosion rate might not be as direct as previously expected.

Table 6

CMC Values of the Inhibitor Model Compounds vs. Surface Saturation Concentrations on Mild Steel

Inhibitor Model Compound	CMC in 1 wt.% NaCl (ppm)	Surface Saturation Concentration in 1 wt.% NaCl (ppm)	Final Corrosion Rate (mm/year)	Inhibition Efficiency
K2-C4	> 2000	150-200	1.15	64%
K2-C8	> 4000	100-150	0.69	79%
K2-C12	116 ± 23	50-100	0.38	88%
K2-C14	50 ± 5	25-50	0.22	93%
K2-C16	5.6 ± 0.9	> 50	0.15	95%

CONCLUSIONS

- Inhibitors having different alkyl tail length were synthesized. ^{1}H-NMR analysis confirmed the desired structure and purity of the inhibitor model compounds.
- Increasing the alkyl tail length of model inhibitor compounds helped the formation of micelles and reduced their CMC values, but this effect was limited by solubility as the tail length increased.
- The presence of CO_2 in solution did not affect the CMC value of the K2-C14 inhibitor used in this research.
- The relationship between CMC and the concentration required to reach maximum efficiency (surface saturation concentrations) was not consistent for different alkyl tail lengths of the tested inhibitors, which shows that the correlation between CMC and reduction in corrosion rate might not be as direct as previously expected.

ACKNOWLEDGMENTS

The author would like to thank the following companies for their financial support: Anadarko, Baker Hughes, BP, Chevron, CNOOC, ConocoPhillips, DNV GL, ExxonMobil, M-I SWACO (Schlumberger), Multi-Chem (Halliburton), Occidental Oil Company, PTT, Saudi Aramco, SINOPEC (China Petroleum) and Total.

Dr. Tangonan from the Department of Chemistry and Biochemistry at Ohio University is thanked for his help in collecting NMR data.

REFERENCES

1. D. A. Jones, *Principles and prevention of corrosion*, 2nd ed. (Upper Saddle River, NJ : Prentice Hall, 1996), p.6.
2. “Chevron Richmond Refinery-Pipe Rupture and Fire,” (Richmond, California: U.S. Chemical Safety and Hazard Investigation Board).
3. X. Wen, P. Bai, B. Luo, S. Zheng, and C. Chen, “Review of recent progress in the study of corrosion products of steels in a hydrogen sulphide environment,” *Corrosion Science*, vol. 139 (2018): pp. 124–140.
4. A. Kahyarian, M. Singer, and S. Nesic, “Modeling of uniform CO_2 corrosion of mild steel in gas transportation systems: A review,” *Journal of Natural Gas Science and Engineering*, vol. 29 (2016): pp. 530–549.
5. L. D. Paolinelli, A. Rashedi, J. Yao, and M. Singer, “Study of water wetting and water layer thickness in oil-water flow in horizontal pipes with different wettability,” *Chemical Engineering Science*, vol. 183 (2018): pp. 200–214.
6. A. Rashedi, “A Study of Surface Wetting in Oil-Water Flow in Inclined Pipeline,” Ohio University, 2016.
7. H. Mansoori, R. Mirzaee, and A. Mohammadi, “Pitting Corrosion Failures of Natural Gas Transmission Pipelines,” International Petroleum Technology Conference (Beijing, China, IPTC: 2013).
8. C. G. Dariva and A. F. Galio, “Corrosion Inhibitors-Principles, Mechanisms and Applications,” in *Developments in Corrosion Protection*, In Tech, (2014): pp. 365–379.
9. H. Mansoori, R. Mirzaee, A. H. Mohammadi, and F. Esmaeilzadeh, “Acid Washes, Oxygenate Scavengers Work Against Gas Gathering Failures,” *Oil and Gas Journal*, vol. 111, no. 7, (2013): pp. 106–111.

10. Z. Belarbi *et al.*, “Volatile Corrosion Inhibitor for Prevention of Black Powder in Sales Gas Pipelines,” CORROSION 2018, Paper no.10962 (Phoenix, Arizona: NACE, 2018).
11. Z. Belarbi, F. Farelas, M. Singer, and S. Nešić, “Role of Amines in the Mitigation of CO_2 Top of the Line Corrosion,” *CORROSION*, vol. 72, no. 10, (2016): pp. 1300–1310.
12. V. Pandarinathan, K. Lepková, S. I. Bailey, T. Becker, and R. Gubner, “Adsorption of Corrosion Inhibitor 1-Dodecylpyridinium Chloride on Carbon Steel Studied by in Situ AFM and Electrochemical Methods,” *Ind. Eng. Chem. Res.*, vol. 53, no. 14, (2014): pp. 5858–5865.
13. Y. Zhu, M. L. Free, R. Woollam, and W. Durnie, “A review of surfactants as corrosion inhibitors and associated modeling,” *Progress in Materials Science*, vol. 90, (2017): pp. 159–223.
14. J. M. D. Olivo, B. Brown, and S. Nesic, “Modeling of Corrosion Mechanisms in the Presence of Quaternary Ammonium Chloride and Imidazoline Corrosion Inhibitors,” CORROSION 2016, Paper no.7406 (Houston, Texas: NACE: 2016).
15. E. A. Badr, “Inhibition effect of synthesized cationic surfactant on the corrosion of carbon steel in 1M HCl,” *Journal of Industrial and Engineering Chemistry*, vol. 20, no. 5, (2014): pp. 3361–3366.
16. C. Zuriaga-Monroy, R. Oviedo-Roa, L. E. Montiel-Sánchez, A. Vega-Paz, J. Marín-Cruz, and J.-M. Martínez-Magadán, “Theoretical Study of the Aliphatic-Chain Length’s Electronic Effect on the Corrosion Inhibition Activity of Methylimidazole-Based Ionic Liquids,” *Ind. Eng. Chem. Res.*, vol. 55, no. 12, (2016): pp. 3506–3516.
17. C. Zuriaga-Monroy, R. Oviedo-Roa, L. E. Montiel-Sánchez, A. Vega-Paz, J. Marín-Cruz, and J.-M. Martínez-Magadán, “Theoretical Study of the Aliphatic-Chain Length’s Electronic Effect on the Corrosion Inhibition Activity of Methylimidazole-Based Ionic Liquids,” *Ind. Eng. Chem. Res.*, vol. 55, no. 12, pp. 3506–3516, Mar. 2016.
18. R. Fuchs-Godec, “The adsorption, CMC determination and corrosion inhibition of some N-alkyl quaternary ammonium salts on carbon steel surface in 2M H_2SO_4,” *Colloids and Surfaces A: Physicochemical and Engineering Aspects*, vol. 280, no. 1, (2006): pp. 130–139.
19. J. M. D. Olivo, D. Young, B. Brown, and S. Nesic, “Effect of Corrosion Inhibitor Alkyl Tail Length on the Electrochemical Process Underlying CO_2 Corrosion of Mild Steel,” CORROSION 2018, Paper no.11537 (Phoenix, Arizona, NACE: 2018).
20. Mm. A. A. Malik, M. A. Hashim, F. Nabi, S. A. AL-Thabaiti, and Z. Khan, “Anti-corrosion Ability of Surfactants: A Review,” *International Journal of Electrochemical Science*, vol. 6, (2011): pp. 1927–1948.
21. M. E. Achouri, Y. Bensouda, H. M. Gouttaya, B. Nciri, L. Perez, and M. Infante, “Gemini Surfactants of the Type 1,2-ethanediyl bis-(dimethylalkylammonium bromide),” *Tenside Surfactants Detergents*, vol. 38, no. 4, (2011): pp. 208–215.
22. M. L. Free, “Understanding the effect of surfactant aggregation on corrosion inhibition of mild steel in acidic medium,” *Corrosion Science*, vol. 44, no. 12, (2002): pp. 2865–2870.
23. H. Z. Sommer, H. I. Lipp, and L. L. Jackson, “Alkylation of amines. General exhaustive alkylation method for the synthesis of quaternary ammonium compounds,” *J. Org. Chem.*, vol. 36, no. 6, (1971): pp. 824–828.
24. M. S. Gibson, “The introduction of the amino group,” *The Amino Group (1968), (*John Wiley & Sons, Ltd, 2010), p. 37–77.
25. J. Drelich, C. Fang, and C. L. White, “Measurement of Interfacial Tension in Fluid-Fluid Systems,” in *Encyclopedia of Surface and Colloid Science*, (Houghton, Michigan, Michigan State University, 2002), p. 3158–3163.
26. H. Zuidema and G. Waters, “Ring Method for the Determination of Interfacial Tension,” *Ind. Eng. Chem. Anal. Ed.*, vol. 13, no. 5, (1941): pp. 312–313.
27. K. W. Bewig and W. A. Zisman, “The Wetting of Gold and Platinum by Water,” *J. Phys. Chem.*, vol. 69, no. 12, (1965): pp. 4238–4242.
28. T. Murakawa, S. Nagaura, and N. Hackerman, “Coverage of iron surface by organic compounds and anions in acid solutions,” *Corrosion Science*, vol. 7, no. 2, (1967): pp. 79–89.